Physico-Chemical Doubly Confinement and Chloride Ion Activation Enabled Two-Electron Conversion Zn-I_2 Battery

Wenting Feng [1], Xinru Wei [2], Junwei Han [1], Chenyu Ma [2], Yiming Sun [2], Peicai Li [2], Debin Kong [2,*], Linjie Zhi [1,2]

[1] School of Materials Science and Engineering, Advanced Chemical Engineering and Energy Materials Research Center, China University of Petroleum (East China), Qingdao 266580, P. R. China

[2] College of New Energy, China University of Petroleum (East China), Qingdao 266580, P. R. China

*Corresponding Author Email: kongdb@upc.edu.cn

Abstract. Aqueous zinc-iodine (Zn-I_2) batteries are emerging as promising alternatives to lithium-ion batteries, boasting high theoretical capacity along with abundant natural resources and environmental safety. The redox chemistry of iodine in these batteries, exploiting its multiple valence states, offers potential for intricate multi-electron conversion reactions. However, challenges such as iodine's volatility and poor conductivity hinder direct use as a cathode material, impacting battery efficiency and cycle life. Strategies involving physico-chemical adsorption in carbon-based hosts show promise by enhancing iodine loading and stability. A synthesized porous carbon material, enriched with carbonate functional groups, achieved a remarkable iodine loading efficiency of 66.69 wt.%. When applied as the cathode in a Zn-I_2&Cl battery configuration, incorporating two-electron conversion of iodine via chloride ions activation, it demonstrated a specific capacity exceeding 200mAh g-1 at 1C, with stable cycling performance over 600 cycles at 5C. This approach underscores the critical role of tailored cathode materials in advancing Zn-I_2 battery technology.

Keywords: Zn-I_2 battery, porous carbon, physico-chemical adsorption, halogen ion, activation.

1. Introduction

Aqueous zinc-iodine (Zn-I_2) batteries represent a promising advancement in energy storage technology, positioned as viable alternatives to lithium-ion batteries due to their high theoretical capacity, substantial energy density, abundant natural resources, inherent safety, and environmental friendliness. [1-3] The redox electrochemical reaction involving iodine in Zn-I_2 batteries has garnered significant interest due to its capability to generate substantial voltage potentials and achieve theoretical capacities of up to 211 mAh g^{-1}. [4-6] Furthermore, iodine's multiple valence states (ranging from -1 to +7) render it particularly intriguing for potentially intricate multi-electron conversion reactions. [7] Typically, cathodic reactions in these batteries involve single-electron transfer I^0/I^- reactions. [8-10] Theoretically, by facilitating iodine-positive transitions at the cathode, two distinct voltage platforms can be realized: I^-/I^0 and I^0/I^+. [11-12] This innovative approach has the potential to double the battery's capacity and significantly enhance its energy density.

However, the widespread adoption of Zn-I_2 batteries is hindered by several challenges. Specifically, the volatility and poor conductivity of I_2 make it unsuitable for direct use as a cathode material. Additionally, numerous critical issues associated with iodine conversion, such as slow reaction kinetics, the multi-iodine species shuttle effect, and instability of the zinc anode, collectively contribute to low coulombic efficiency, and poor capacity and cycle life, thereby limiting their practical application. [13-15] A classical approach involves confining active I_2 within the porous structure of a host material through physical adsorption. [16-17] However, this method has limitations, with I_2 content typically constrained to 20 wt.% to 50 wt.%, and the interaction between the host material and polyiodide species often proving insufficient. Therefore, the strategic design and development of cathode materials are crucial for enhancing the electrochemical performance of Zn-I_2 batteries. [18]

Carbon-based materials have been extensively utilized as host materials due to their exceptional electrical conductivity, high specific surface area, tunable pore structure, excellent chemical inertness, and thermal stability. [19-20] However, effectively and stably incorporating active iodine into these hosts remains a critical factor limiting their performance. The simple adsorption strength between host and I_2 is often insufficient, leading to the loss of iodine during conversion reactions in Zn-I_2 batteries. Physical properties such as specific surface area and pore structure significantly influence the loading of active I_2 in carbon materials. Moreover, chemical modification of carbon materials can enhance the binding of substrates to iodine species, thereby addressing these limitations and improving overall battery performance.

Hence, we propose a strategy to enhance Zn-I_2 battery performance through physico-chemical adsorption, employing a carbon host enriched with a robust pore structure and chemical constraints. A porous carbon (PC) material with ample pore structure was synthesized using $MnCO_3$ as an inorganic salt template and methyl cellulose (MC) as a carbon source. Leveraging the chemical inheritance of carbonates, the surface of this porous carbon was endowed with abundant carbonate functional groups, significantly boosting iodine adsorption with a high loading efficiency of 66.69 wt.%. This PC@I_2 material was employed as the anode, activating I^+ by introducing heterogeneous halogen chlorine into the electrolyte. This innovation enabled the development of a high specific capacity Zn-I_2&Cl battery. Specifically, a specific capacity exceeding 200 was achieved at a current density of 1C (1C=211 mA g^{-1}). With the improved kinetics provided by chloride ions, the battery demonstrated stable cycling performance, enduring over 600 cycles at a high current density of 5C.

2. Results and Discussion

2.1. Chemisorption and Kinetic Mechanism Study of the Carbon Host to Iodine Species

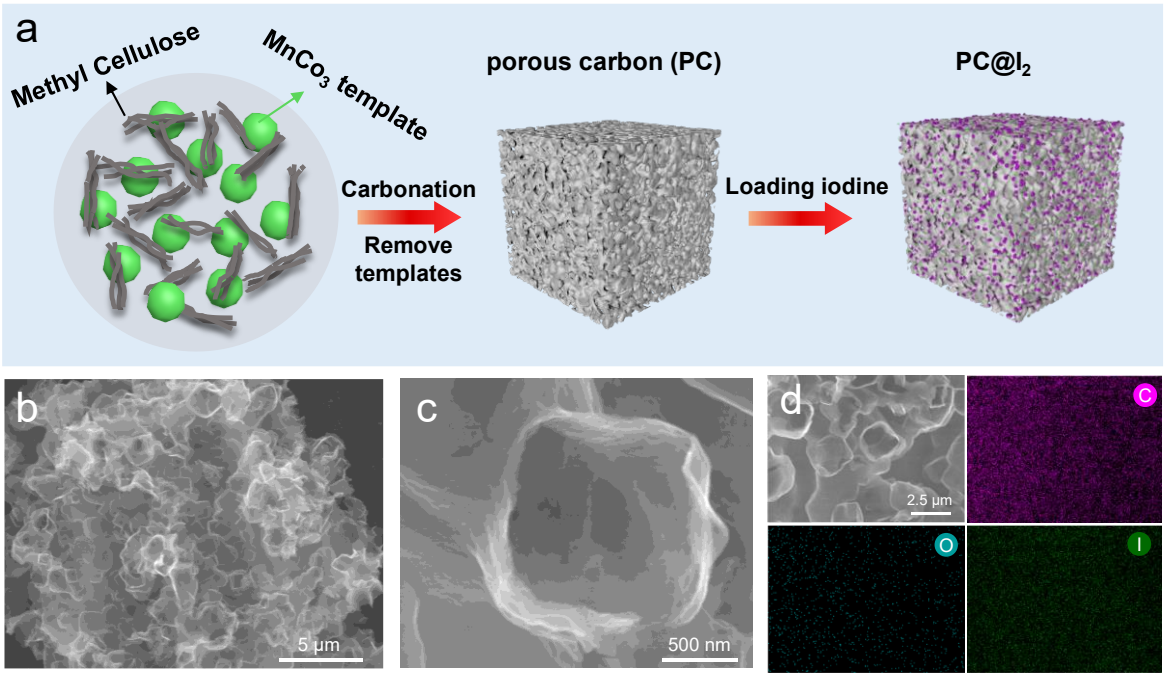

Figure 1. Morphological and structural characterization of PC@I_2. (a) Schematic illustration of the synthesis of porous carbon (PC) via the $MnCO_3$ template method and iodine loading (PC@I_2). (b) SEM image of PC. (c) Enlarged SEM image of PC. (d) SEM image of PC@I_2 and corresponding energy dispersive spectroscopy (EDS) elemental mappings of C, O, and I.

The synthesis process for the PC and PC@I_2 materials is outlined in Figure 1a. Initially, methyl cellulose (MC) was used as the carbon source, while manganese carbonate ($MnCO_3$) served as the inorganic salt template. This combination enabled the creation of cubic porous carbon materials with an extensive pore structure through a series of simple steps, including mixing, carbonization, and the

subsequent removal of the template. After forming the porous carbon structure, iodine species were incorporated onto the porous carbon using an impregnation adsorption method, obtaining the PC@I_2 electrode material. Figure 1b shows the SEM morphology of the PC, which maintains the cubic shape of the $MnCO_3$ template. The cubic pores measure approximately 1 μm on each side, and their interconnected nature facilitates efficient material and charge transfer within the electrode. Enlarged SEM images (Figure 1c) reveal that the walls of the cubic porous carbon exhibit folds and wrinkles, which enhance the specific surface area and provide additional active sites for iodine loading. EDS elemental mappings confirm a uniform distribution of iodine throughout the porous carbon matrix. Additionally, the inorganic salt templating method introduces numerous carbonate functional groups onto the carbon material, which are crucial for improving the immobilization of iodine species. This strategic design of the porous carbon and effective iodine loading significantly enhance the performance of Zn-I_2 batteries via the improved structural and chemical feature.

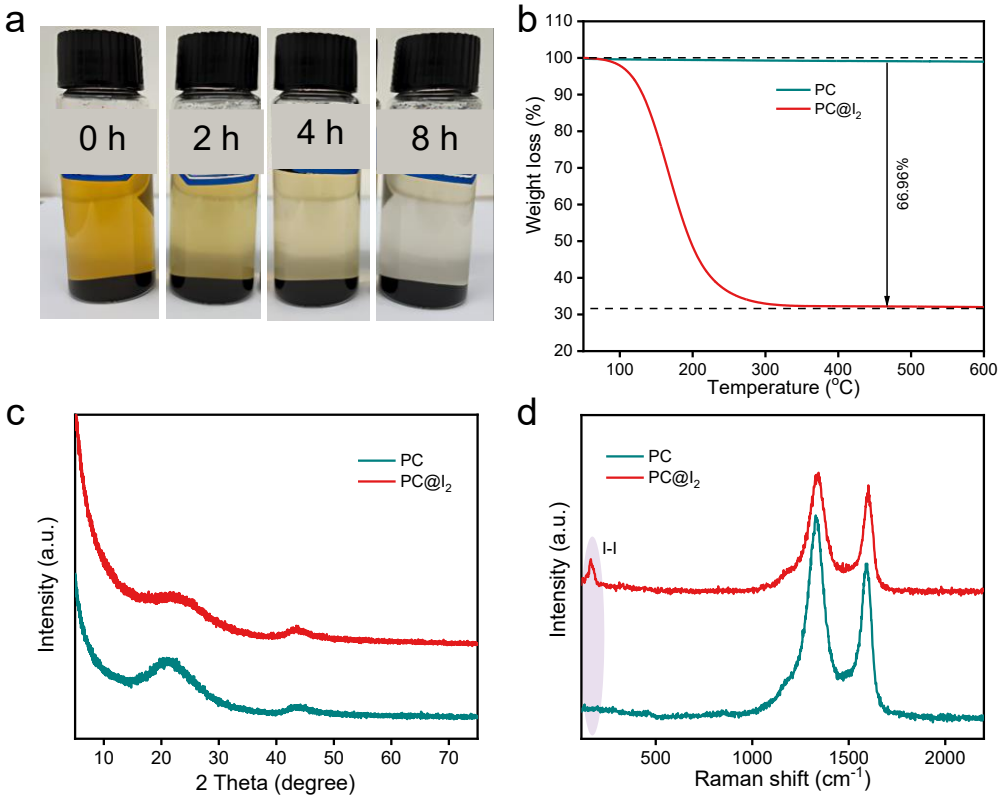

Figure 2. Fundamental characterization of PC@I_2. (a) Photographs of PC adsorption of iodine at different times. (b) Thermogravimetric analysis (TGA) curves of PC and PC@I_2. (c) X-ray diffraction (XRD) pattern of PC and PC@I_2. (d) Raman spectra of PC and PC@I_2.

In order to elucidate the strong adsorption properties of PC matrix to iodine species, the enhanced adsorption capacity of PC host to iodine species was studied by visual adsorption test (Figure 2a). When PC was immersed in an aqueous solution of iodine, the solution gradually became clearer over time. After 8 hours, the iodine solution was nearly transparent, demonstrating the exceptional adsorption capability of the porous carbon host for iodine species. This observation confirms the effective interaction and strong adsorption of iodine by the PC matrix, particularly in the aqueous environment typical of Zn-I_2 batteries. Further analysis of the iodine loading capacity in the PC was performed using TGA (Figure 2b). By comparing the weight loss data of PC and PC@I_2 under identical conditions, the specific iodine loading capacity was determined to be 66.69 wt%, this indicates that porous carbon host exhibits more active sites to adsorb iodine species. This value significantly exceeds the typical iodine loading limits of most carbon substrates. Such a high loading capacity is crucial for enhancing the energy density of Zn-I_2 batteries, as it allows for a substantial increase in the amount of active iodine species available for electrochemical reactions. The improved

adsorption and high iodine loading contribute to more efficient and effective battery performance, addressing key challenges in the development of high-energy-density Zn-I_2 batteries.

The XRD patterns of PC and PC@I_2 show that there are no obvious peaks of iodine, which indicates that iodine is uniformly adsorbed without obvious large particle aggregation (Figure 2c). This uniform distribution is mainly attributed to the abundant oxygen-containing functional groups in porous carbon prepared by $MnCO_3$ template method, which produce chemical forces on iodine. This is further confirmed by Raman spectroscopy, which shows a vibrational stretching peak near ~160 cm^{-1}, which indicates the presence of iodine (Figure 2d). The other two peaks located at ~1340 and 1600 cm^{-1} are observed, which correspond to the D-band (disordered carbon) and the G-band (graphitized carbon) of porous carbon matrix, respectively. [20] Surprisingly, the tight interaction between iodine and carbon substrate promotes rapid electron transport and enhances the reaction kinetics of the Zn-I_2 battery, thus improving the performance and efficiency of the battery.

2.2. Storage Mechanism and Electrochemical Performance

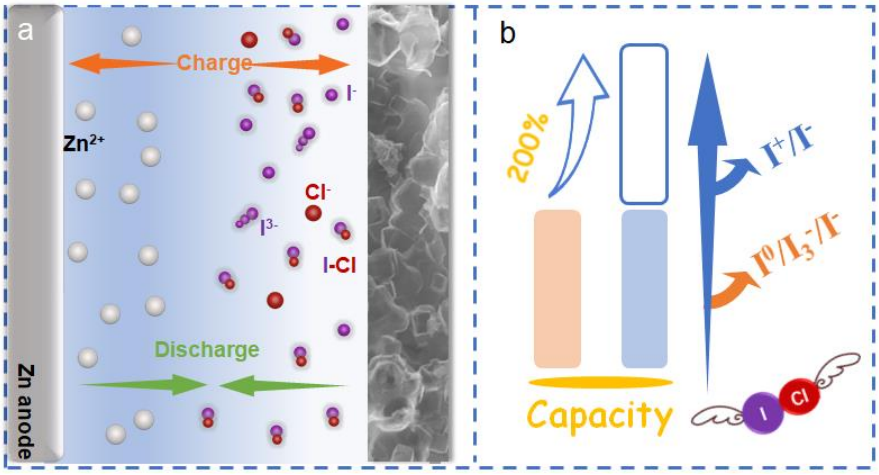

Figure 3. Mechanism diagram of ICl conversion reaction in Zn-I_2 batteries. (a) Charge and discharge processes schematic of Zn-I_2 battery with Cl species. (b) The illustration of the possible capacity enhancements of ICl conversion.

The introduction of heterogeneous halogens into Zn-I_2 batteries has proven to be effective in activating I^+ conversion. [21-23] To facilitate this process, $AlCl_3$ was incorporated into the electrolyte to induce I^+ conversion. As illustrated in Figure 3a, we developed a Zn-I_2 battery system containing chlorine to facilitate the effective conversion of I^- into I^+ (as ICl), with the electrodes labeled as PC@I_2&Cl^-. During the electrochemical operation of this system, the following reactions take place at the zinc anode electrode:

$Zn^{2+} + 2e^- \leftrightarrow Zn$

And two reactions of the iodine species conversion occur at the cathode:

$2I^- \leftrightarrow I_2 + 2e^-$

$I_2 + 2Cl^- \leftrightarrow 2ICl + 2e^-$

Overall, the total reactions in the battery system are as follows:

$Zn^{2+} + 2I^- \rightarrow Zn + I_2$, E = 1.29 V

$Zn^{2+} + I_2 + 2Cl^- \rightarrow Zn + 2ICl$, E = 1.83 V

Additionally, the two-electron transfer mechanism is expected to double the theoretical capacity to 422 mAh g^{-1}. In terms of energy density, a significant increase of over 200% compared to the original value can be achieved, thanks to the higher potential of the triggered conversion plateau (Figure 3b). These reactions underscore the enhanced performance and potential improvements in energy density and efficiency made possible by incorporating heterogeneous halogens into the zinc-iodine battery system.

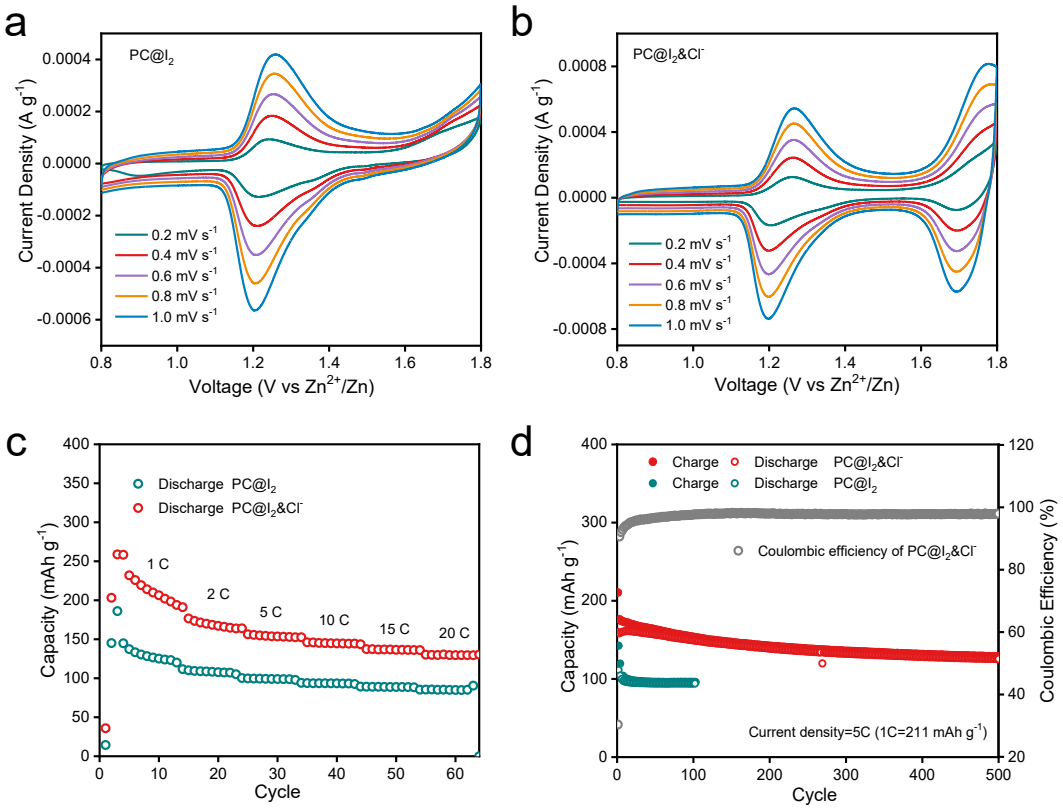

Figure 4. Electrochemical performance of PC@I_2&Cl^- electrode. (a) CV curves of PC@I_2 electrode at different scan rate from 0.2 to 1.0 mV s^{-1}. (b) CV curves of PC@I_2&Cl^- electrode at different scan rate from 0.2 to 1.0 mV s^{-1}. (c) Rate capability of PC@I_2 and PC@I_2&Cl^- electrodes. (d) Cycling performance of PC@I_2 and PC@I_2&Cl^- electrodes at 5C (1C=211mA g^{-1}).

Electrochemical performances of Zn-I_2 batteries with PC@I_2 and PC@I_2&Cl^- electrodes are evaluated based on cyclic voltammetry (CV) tests. Figure 4a shows the CV profiles of Zn-I_2 battery with PC@I_2 electrode at different scan rate from 0.2 to 1.0 mV s^{-1}. The Zn-I_2 battery with PC@I_2 electrode depicts a well-known pair of redox peaks at 1.20/1.25 V, corresponding to the single redox stage of I^-/I^0 couple. In sharp contrast, two well defined pairs of redox peaks can be identified in the Zn-I_2 battery with PC@I_2&Cl^- electrode. Apart from the familiar couple, a new redox pair is detected at 1.70/1.75 V (Figure 4b). This showcase indicates an activated new reversible chemistry. Specifically, the PC@I_2&Cl^- electrode demonstrates reversible capacities of 210, 168, 154, 145, 137, and 130 mAh g^{-1} at current densities of 1C, 2C, 5C, 10C, 15C, and 20C, respectively (Figure 4c). These values are significantly higher compared to those of the PC@I_2 electrode, which shows capacities of 128, 109, 99, 94, 89, and 85 mAh g^{-1} at the same current densities. Figure 4d illustrates the cycling performance of the electrodes at a current density of 5C. The PC@I_2&Cl^- electrode retains a high reversible capacity of 126 mAh g^{-1} after 500 cycles, demonstrating its excellent cycle stability and performance. In contrast, the PC@I_2 electrode exhibits a lower capacity of 94 mAh g^{-1} under the same conditions, indicating a relatively less stable cycling performance. This comparison highlights the superior durability and capacity retention of the PC@I_2&Cl^- electrode over extended cycling.

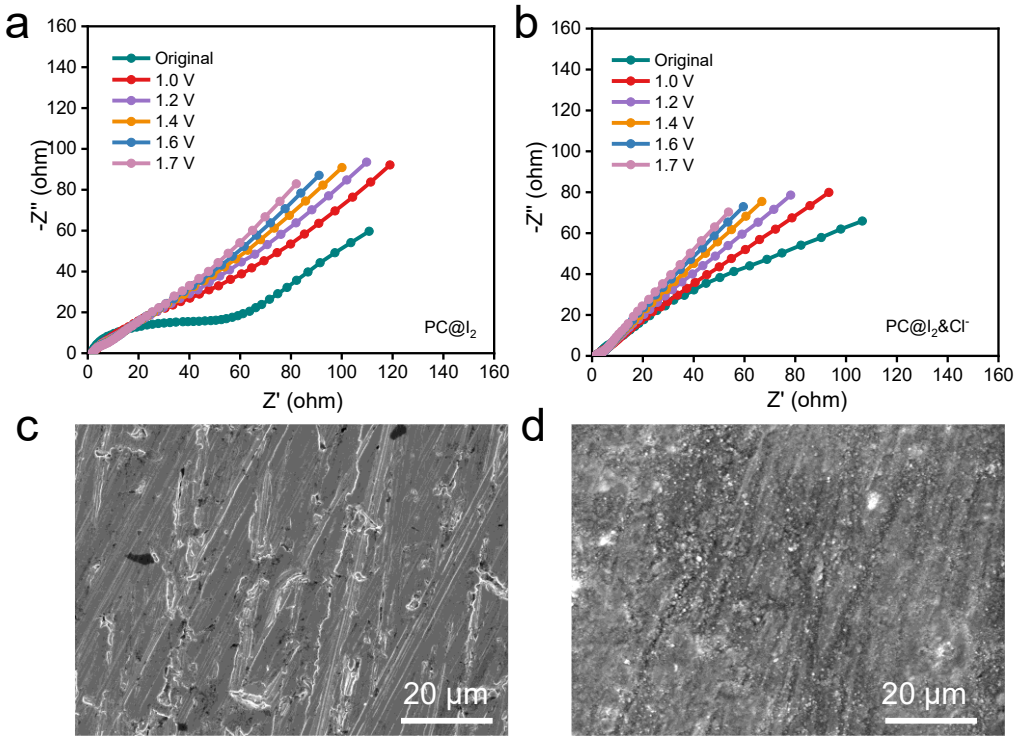

Figure 5. (a) In situ EIS of PC@I_2 electrode. (b) In situ EIS of PC@I_2&Cl^- electrode. (c) SEM images of Zn anode of Zn-I_2 battery with PC@I_2 electrode after 50 cycles. (d) SEM images of Zn anode of Zn-I_2 battery with PC@I_2&Cl^- electrode after 50 cycles.

To investigate the interfacial charge transfer processes at different discharge states, in situ electrochemical impedance spectroscopy (EIS) was employed to monitor resistance variations throughout the redox reactions of the PC@I_2&Cl^- and PC@I_2 electrodes. The analysis revealed that the PC@I_2&Cl^- electrode exhibited consistently lower charge transfer resistance compared to the PC@I_2 electrode, both in its initial state and during the charging process (ranging from 1.0 V to 1.7 V). This reduction in resistance confirms that the PC@I_2&Cl^- electrode facilitates more rapid kinetics for the redox reactions and more efficient interfacial charge transfer. These findings, illustrated in Figure 5a and 5b, highlight the superior performance of the PC@I_2&Cl^- electrode in supporting faster and more effective charge exchange processes compared to the PC@I_2 electrode.

The corrosion of Zn anode surface was further studied to verify the inhibition of PC@I_2&Cl^- electrode to the shuttle effect of polyiodide species. Figure 5c and 5d display the surface deposition morphology of the Zn anode in Zn-I_2 batteries with PC@I_2&Cl^- and PC@I_2 electrodes after 50 cycles at a current density of 5C. The images reveal that the PC@I_2&Cl^- electrode effectively prevents the interaction between polyiodides and the Zn anode, thereby promoting stable Zn ion deposition. Furthermore, the enhanced reaction kinetics and reversible conversion facilitated by the PC@I_2&Cl^- electrode improve the utilization efficiency of the active iodide species. This leads to reduced corrosion of the Zn anode surface and contributes to the overall superior electrochemical performance of the Zn-I_2 batteries.

3. Conclusion

In summary, we synthesized porous carbon substrates with a rich pore structure and abundant oxygen-containing functional groups using an inorganic salt templating method. Iodine was adsorbed onto the PC substrates as the initial active material. The PC substrate with extensive pore structure adsorbed up to 66.69 wt% of I_2, effectively minimizing iodine species loss and inhibiting polyiodide shuttling through the strong chemical interactions of the oxygenated functional groups. Additionally, the introduction of heterogeneous Cl^- into the battery system facilitated the efficient conversion of I^+. The PC@I_2&Cl^- electrode system demonstrated higher specific capacity and energy density, along

with excellent cycling stability, compared to the PC@I_2 electrode. It is believed that the physicochemical dual-constraint synergistic activation strategy for heterogeneous halogens in this work offers a valuable approach for advancing high-performance Zn-I_2 batteries.

4. Material and Methods

(1) Material Synthesis

Synthesis of PC material: Methyl cellulose (MC) and manganese carbonate (MnCO3) were combined in a mass ratio of 1:5, then placed in a tube furnace. The mixture was heated to 800°C at a rate of 5°C/min, maintained at this temperature for 2 hours and processed under an argon atmosphere for inert protection. After cooling, the black precursor was washed with 1 M HCl for 1 hour, then filtered and vacuum-dried at 100°C overnight to yield the final porous carbon (PC) material.

Synthesis of PC@I_2 material: A specific quantity of PC material was immersed in a supersaturated aqueous iodine solution and allowed to adsorb for 12 hours. The mixture was then filtered, and dried overnight in a vacuum oven at 60°C to produce the PC@I_2 material.

(2) Material Characterization

Morphology of the PC PC@I_2 and Zn anode materials were investigated by using scanning electron microscope (SEM, SU8010). Structure characterizations of the PC and PC@I_2 materials were recorded by using powder X-ray diffractometer (XRD, X`Pert PRO MPD) and Raman test (HORIBA HR Evolution with 532 nm wavelength). The mass loading of I_2 in PC was calculated based on thermogravimetric analyses (TGA, WRT-12) in nitrogen atmosphere.

(3) Electrochemical Evaluation

Assembling of Zn-I_2 batteries with PC@I_2 and PC@I_2&Cl^- electrodes: The electrochemical properties of the electrode materials were evaluated at room temperature. Cathodes were prepared by mixing the PC@I_2 material, Super P, and polyvinylidene fluoride (PVDF) in N-methyl-2-pyrrolidone (NMP) solvent at a mass ratio of 8:1:1, with an active material loading of approximately 1.5 mg cm^{-2}. Fresh zinc metal foil was used as the anodes, and a 2 M $ZnSO_4$ solution was employed as the electrolyte, with 60 μL of electrolyte used per battery. For the PC@I_2&Cl^- electrodes, 1 M $AlCl_3$ was added to the electrolyte. A Whatman glass microfibre filter served as the separator. The CR2032 button cells were assembled in-house.

Electrochemical tests of Zn-I_2 battery: Rate and cycling performance were performed using a battery measurement system (Land CT3002A). Cyclic voltammetry (CV) and Electrochemical impedance spectroscopy (EIS) were performed using an GAMRY electrochemical workstation at different frequencies from 1000000 Hz to 0.01 Hz.

Acknowledgements

This work was financially supported by National Natural Science Foundation of China (U20A20131, 52172040, 92372204), Taishan Scholar Project of Shandong Province (ts202208832, tsqn202211086).

References

[1] Jin, X.; Song, L.; Dai, C.; Xiao, Y.; Han, Y.; Li, X.; Wang, Y.; Zhang, J.; Zhao, Y.; Zhang, Z.; Chen, N.; Jiang, L.; Qu, L., A Flexible Aqueous Zinc-Iodine Microbattery with Unprecedented Energy Density. Adv. Mater. 2022, 34, e2109450.

[2] Chen, H.; Li, X.; Fang, K.; Wang, H.; Ning, J.; Hu, Y., Aqueous Zinc-Iodine Batteries: From Electrochemistry to Energy Storage Mechanism. Adv. Energy Mater. 2023, 13, 2302187.

[3] Li, W.; Wang, D., Conversion-Type Cathode Materials for Aqueous Zn Metal Batteries in Nonalkaline Aqueous Electrolytes: Progress, Challenges, and Solutions. Adv. Mater. 2023, 2304983.

[4] Huang, L.; Li, W.; Wei, F.; Ke, S.; Chen, H.; Jing, C.; Cheng, J.; Liu, S., Hierarchical porous covalent organic framework nanosheets with adjustable large mesopores. Chem. 2024, 10, 1-14.

[5] Zhu, L.; Guan, X.; Fu, Y.; Zhang, Z.; Li, Y.; Mai, Q.; Zhang, C.; Yuan, Z.; Wang, Y.; Li, P.; Li, H.; Su, D.; Jia, B.; Yu, H.; Sun, Y.; Ma, T., Integrated Trap-Adsorption-Catalysis Nanoreactor for Shuttle-Free Aqueous Zinc-Iodide Batteries. Adv. Funct. Mater. 2024, 2409099.

[6] Hu, Z.; Wang, X.; Du, W.; Zhang, Z.; Tang, Y.; Ye, M.; Zhang, Y.; Liu, X.; Wen, Z.; Li, C. C., Crowding Effect-Induced Zinc-Enriched/Water-Lean Polymer Interfacial Layer Toward Practical Zn-Iodine Batteries. ACS Nano 2023, 17, 23207-23219.

[7] Zou, Y.; Liu, T.; Du, Q.; Li, Y.; Yi, H.; Zhou, X.; Li, Z.; Gao, L.; Zhang, L.; Liang, X., A four-electron Zn-I2 aqueous battery enabled by reversible I-/I2/I+ conversion. Nat. Commun. 2021, 12, 170.

[8] Li, P.; Li, X.; Guo, Y.; Li, C.; Hou, Y.; Cui, H.; Zhang, R.; Huang, Z.; Zhao, Y.; Li, Q.; Dong, B.; Zhi, C., Highly Thermally/Electrochemically Stable I−/I3− Bonded Organic Salts with High I Content for Long-Life Li–I2 Batteries. Adv. Energy Mater. 2022, 12, 2103648.

[9] Wang, K.; Li, H.; Xu, Z.; Liu, Y.; Ge, M.; Wang, H.; Zhang, H.; Lu, Y.; Liu, J.; Zhang, Y.; Tang, Y.; Chen, S., An Iodine-Chemisorption Binder for High-Loading and Shuttle-Free Zn–Iodine Batteries. Adv. Energy Mater. 2024, 14, 2304110.

[10] Yang, J.-L.; Liu, H.-H.; Zhao, X.-X.; Zhang, X.-Y.; Zhang, K.-Y.; Ma, M.-Y.; Gu, Z.-Y.; Cao, J.-M.; Wu, X.-L., Janus Binder Chemistry for Synchronous Enhancement of Iodine Species Adsorption and Redox Kinetics toward Sustainable Aqueous Zn–I2 Batteries. J. Am. Chem. Soc. 2024, 146, 6628-6637.

[11] Bi, S.; Wang, H.; Zhang, Y.; Yang, M.; Li, Q.; Tian, J.; Niu, Z., Six-Electron-Redox Iodine Electrodes for High-Energy Aqueous Batteries. Angew. Chem. Int. Ed. 2023, 62, e202312982.

[12] Li, X.; Wang, Y.; Chen, Z.; Li, P.; Liang, G.; Huang, Z.; Yang, Q.; Chen, A.; Cui, H.; Dong, B.; He, H.; Zhi, C., Two-Electron Redox Chemistry Enabled High-Performance Iodide-Ion Conversion Battery. Angew. Chem. Int. Ed. 2022, 61, e202113576.

[13] Li, Z.; Cao, W.; Hu, T.; Hu, Y.; Zhang, R.; Cui, H.; Mo, F.; Liu, C.; Zhi, C.; Liang, G., Deploying Cationic Cellulose Nanofiber Confinement to Enable High Iodine Loadings Towards High Energy and High-Temperature Zn-I2 Battery. Angew. Chem. Int. Ed. 2023, 63, e202317652.

[14] Chen, Z.; Wang, F.; Ma, R.; Jiao, W.; Li, D.; Du, A.; Yan, Z.; Yin, T.; Yin, X.; Li, Q.; Zhang, X.; Yang, N.; Zhou, Z.; Yang, Q.-H.; Yang, C., Molecular Catalysis Enables Fast Polyiodide Conversion for Exceptionally Long-Life Zinc–Iodine Batteries. ACS Energy Lett. 2024, 9, 2858-2866.

[15] He, J.; Mu, Y.; Wu, B.; Wu, F.; Liao, R.; Li, H.; Zhao, T.; Zeng, L., Synergistic effects of Lewis acid–base and Coulombic interactions for high-performance Zn–I2 batteries. Energy Environ. Sci. 2024, 17, 323-331.

[16] He, J.; Hong, H.; Hu, S.; Zhao, X.; Qu, G.; Zeng, L.; Li, H., Chemisorption effect enables high-loading zinc-iodine batteries. Nano Energy 2024, 119, 109096.

[17] Hu, T.; Zhao, Y.; Yang, Y.; Lv, H.; Zhong, R.; Ding, F.; Mo, F.; Hu, H.; Zhi, C.; Liang, G., Development of Inverse-Opal-Structured Charge-Deficient Co9S8@nitrogen-Doped-Carbon to Catalytically Enable High Energy and High Power for the Two-Electron Transfer I+/I- Electrode. Adv. Mater. 2024, 36, e2312246.

[18] Li, X.; Li, M.; Huang, Z.; Liang, G.; Chen, Z.; Yang, Q.; Huang, Q.; Zhi, C., Activating the I0/I+ redox couple in an aqueous I2–Zn battery to achieve a high voltage plateau. Energy Environ. Sci. 2021, 14, 407-413.

[19] Feng, W. T.; Feng, N. Y.; Liu, W.; Cui, Y. P.; Chen, C.; Dong, T. T.; Liu, S.; Deng, W. Q.; Wang, H. L.; Jin, Y. C., Liquid-State Templates for Constructing B, N, Co-Doping Porous Carbons with a Boosting of Potassium-Ion Storage Performance. Adv. Energy Mater. 2021, 11, 2003215.

[20] Feng, W. T.; Cui, Y. P.; Liu, W.; Wang, H. L.; Zhang, Y.; Du, Y. X.; Liu, S.; Wang, H. L.; Gao, X.; Wang, T. Q., Rigid-Flexible Coupling Carbon Skeleton and Potassium-Carbonate-Dominated Solid Electrolyte Interface Achieving Superior Potassium-Ion Storage. ACS Nano 2020, 14, 4938-4949.

[21] Wang, M.; Meng, Y.; Sajid, M.; Xie, Z.; Tong, P.; Ma, Z.; Zhang, K.; Shen, D.; Luo, R.; Song, L.; Wu, L.; Zheng, X.; Li, X.; Chen, W., Bidentate Coordination Structure Facilitates High-Voltage and High-Utilization Aqueous Zn-I2 Batteries. Angew. Chem. Int. Ed. 2024, e202404784.

[22] Liu, T.; Lei, C.; Wang, H.; Yang, W.; He, X.; Liang, X., Triflate anion chemistry for enhanced four-electron zinc-iodine aqueous batteries. Chem. Commun. 2024, 60, 7447-7450.

[23] Zhang, Q.; Ma, Y.; Lu, Y.; Ni, Y.; Lin, L.; Hao, Z.; Yan, Z.; Zhao, Q.; Chen, J., Halogenated Zn2+ Solvation Structure for Reversible Zn Metal Batteries. J. Am. Chem. Soc. 2022, 144, 18435-18443.